Wind and Structures, *Vol. 21, No. 6 (2015) 609-623*
DOI: http://dx.doi.org/10.12989/was.2015.21.6.609

Dynamic reliability analysis of offshore wind turbine support structure under earthquake

Dong-Hyawn Kim*[1], Gee-Nam Lee[1a], Yongjei Lee[2b] and Il-Keun Lee[3c]

[1]*Department of Ocean Science and Engineering, Kunsan National University, Kunsan, 54150, Korea*
[2]*Chang Minwoo Structural Consultants, Seoul, 135-907, Korea*
[3]*Korea Expressway Corporation Research Institute, Gyeonggi, 18489, Korea*

(Received October 7, 2015, Revised November 19, 2015, Accepted November 30, 2015)

Abstract. Seismic reliability analysis of a jacket-type support structure for an offshore wind turbine was performed. When defining the limit state function by using the dynamic response of the support structure, a number of dynamic calculations must be performed in a First-Order Reliability Method (FORM). That means analysis costs become too high. In this paper, a new reliability analysis approach using a static response is used. The dynamic effect of the response is considered by introducing a new parameter called the Peak Response Factor (PRF). The probability distribution of PRF can be estimated by using the peak value in the dynamic response. The probability distribution of the PRF was obtained by analyzing dynamic responses during a set of ground motions. A numerical example is presented to compare the proposed approach with the conventional static response-based approach.

Keywords: offshore wind turbine; support structures; reliability; earthquake; dynamic response; peak response

1. Introduction

In the sea area, there exist ordinary loads such as wave and wind as well as occasional loads such as earthquake, typhoon, and tsunami (Choi *et al*. 2014, Yi *et al*. 2014). Among them, the seismic load can cause the most severe damage to the structures. Recently, more frequent and bigger earthquakes have been observed at sea; therefore, the safety evaluation of the offshore structures under earthquake is very important. The seismic design code in Korea is based on the deterministic approach in which uncertainties in the applied loads and soil properties are considered. These uncertainties must be considered to prevent non-conservative or conservative design so as to achieve an accurate structural evaluation. Many active studies have been conducted to apply the uncertainties of variables to the design in response to the increasing needs of reliability design (Bush and Manuel 2009, Zhang *et al*. 2010). In the existing reliability analysis, the seismic load is converted into a static load that does not account for the frequency

*Corresponding author, Professor, E-mail: welcomed@naver.com
[a] Graduate Student
[b] Senior Associate, Ph.D, PE
[c] Deputy Research Director, Ph.D.

http://www.techno-press.org/?journal=was&subpage=8 ISSN: 1226-6116 (Print), 1598-6225 (Online)

characteristics. Therefore, the calculated probability of failure might not be accurate (Lee and Kim 2011). Reliability analysis with only the static seismic load is not appropriate and an analysis with dynamic seismic load must be conducted. However, the dynamic seismic analysis takes lots of time for repetitive structural analysis on the estimation of the response surface and the reliability analysis. By using the peak response factor (PRF) which is defined as the ratio of dynamic response to static response, the time issue can be solved (Lee and Kim 2014).

In this study, dynamic effects were taken into account in a reliability analysis by using PRF. The seismic load, soil property, and PRF were considered as random variables, and a limit state function was defined by using a response surface. With the response based limit state function, a reliability analysis using the First-Order Reliability Method (FORM) was conducted (Hasofer *et al*. 1974). The random variables other than the normal distribution were defined by the Rackwitz–Fiessler method (Rackwitz and Fiessler 1978). A jacket structure, which has been used for oil drilling for a long time, was used as an example (Nava *et al*. 2014). Latin Hypercube Sampling based Monte Carlo simulation (LHS) was used to verify the proposed method in this study, which requires relatively small sample designs to achieve convergence in failure probability.

2. Theory

2.1 Reliability analysis

The reliability analysis can be divided into three levels according to the designer's requirements. Firstly, sampling based method, the so-called level III approach, gives the most exact failure probability among them. It needs a large number of random samples for design values to calculate the probability of failure. Secondly, level II method gives approximate reliability index from which the failure probability can be found. The last one, level I method, does not give the failure probability directly but tells us whether any given design set satisfies a target failure probability or not by using partial safety factors. Level II is preferred to level III in design practice when a failure probability is required since it takes much shorter calculation time than level III.

2.2 Response surface method

To perform the reliability analysis, a limit state function should be defined by the random variables, and the structural response such as deflection and rotation are considered as dependent variables. When Level II reliability method is used, the limit state function defined by the variables is expressed in the form of an implicit function and this makes the analysis difficult. The Response Surface Method (RSM) can approximate the limit state function as an explicit function to make analysis easier (Scheuller *et al*. 1987). The response surface can be obtained by selecting the sample points in a constant interval from the center, and performing structural analysis from those points. (Khuri and Cornell 1987). Each sample point can be expressed by Eq. (1).

$$\mathrm{X}_i = \mathrm{X}_i^C \pm h_i \sigma_{X_i} I_i, \tag{1}$$

where X_i^C and σ_{X_i} are the mean and standard deviation of variable X_i, respectively, h_i is the expansion width, and I_i is the scattering index.

It is very important to select design points at which structural analysis is done in response surface method. Bucher-Bourgund Design (BBD), Central Composite Design (CCD), and

Saturated Design (SD) have been suggested for response surface based reliability analysis. In this study, SD was used since it is considered to be optimal in this study (Bucher and Bourgund 1987, Bush and Manuel 2009, Haldar and Mahadevan 2000).

2.3 Peak response factor

The dynamic peak response and the joint probability density function $f_{R_p,X}$ are expressed by Eq. (2). Probability of failure, P_f, is a volume of the probability density function in the negative range of limit state function, and can be expressed by Eq. (3).

$$f_{R_p,X} = f_{R_p|X}(r_p|x)\, f_X(x) \tag{2}$$

$$P_f = \int_{g<0} f_{R_p,X}(r_p, x) dr_p dx = \int_{-\infty}^{\infty} f_{R_p|X}(r_p|x) f_X(x) dr_p dx \tag{3}$$

In Eq. (2), f_X is the probability density function of each variable, $f_{R_p|X}$ is the conditional probability density function of the dynamic peak response when the other variable, X, is given. r_p and x are the dynamic peak response and the variable other than r_p. g in Eq. (3) is the limit state function.

The reliability analysis requires repetitive structural analysis until a convergent reliability index is obtained. In general, a static response is used because obtaining the dynamic peak response every time is not easy. In this study, to apply the existing method considering the dynamic effects, the ratio of dynamic peak response (R_p) to static response (R_{st}) was used, as shown in Eq. (4). The ratio, R_n, is called the Peak Response Factor (PRF) (Lee and Kim 2014).

$$R_n = R_p / R_{st} \tag{4}$$

From Eq. (4), the limit state function can be defined by Eq. (5)

$$g(X) = R_{allowable} - R_n R_{st} \tag{5}$$

Expressing the peak response factor, the joint probability density function of variables, and the limit state function on the normal distribution space, the reliability index (β), which is the shortest distance between the origin and the failure surface, can be obtained.

3. Numerical analysis

3.1 Model and environmental condition

A commercial program, ANSYS Ver. 12.0 (Ansys Inc. 2009), was used for modeling and numerical analysis. A 5 MW offshore wind turbine of NREL (National Renewable Energy Laboratory) reference model (Jonkman *et al*. 2009) was used. A jacket type support structure which was designed for the south-west coast wind farm in Korea was used for numerical analysis. A beam element was used for tower and jacket, and the Rotor and Nacelle (RNA) were converted into a concentrated mass on each center of gravity by a joint mass, as shown in Fig. 1(a).

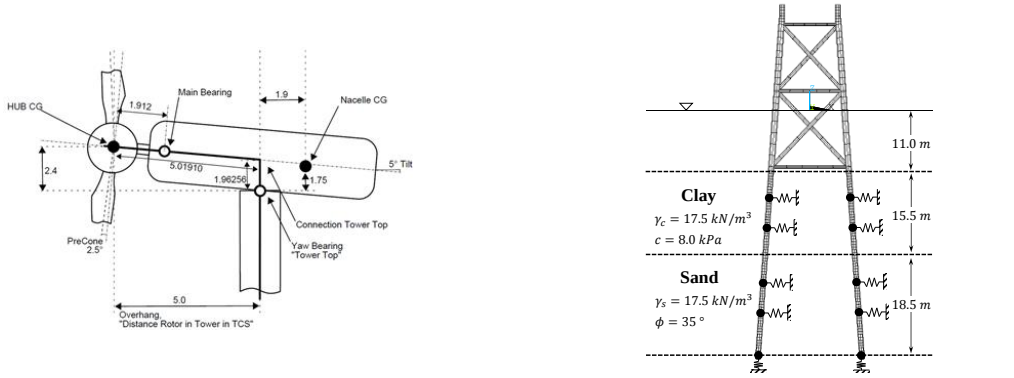

(a) Center of gravity for Hub and Nacelle (b) Finite element model and soil profile

Fig. 1 Offshore Wind Turbine and Soil Profile

3.1.1 Foundation model

As shown in Figure 1(b), the support structure is connected to the foundation composed of cohesive soil and sandy soil, which have a depth of 15.5 m and 18.5 m, respectively. In general, when a load is applied to a structure, a displacement occurs along the load direction and also foundation reaction occurs to resist the displacement. The relationship between the load and displacement is nonlinear. To express the nonlinear effect of the foundation, the API RP 2A (American Petroleum Institute, 2007) recommends nonlinear *p–y* curve between the two.

A *p–y* curve for cohesive soil is listed in Table 1(API, 2007), and the ultimate bearing force (p_u) by Eq. (6) is used for the *p–y* curve. Here, X, c, D, γ, and J are the depth from the surface, undrained shear strength, pile diameter, effective specific weight, and empirical constant, respectively. X_R is a critical depth calculated from Eq. (7). y_c is a parameter of the critical displacement calculated from Eq. (8). ε_c is a constant strain corresponding to a half the maximum stress from the undrained compressive test.

Table 1 p-y curves under cyclic loading

$X > X_R$		$X < X_R$	
p/p_u	y/y_u	p/p_u	y/y_u
0.00	0.0	0.00	0.0
0.23	0.1	0.23	0.1
0.33	0.3	0.33	0.3
0.50	1.0	0.50	1.0
0.72	3.0	0.72	3.0
0.72	∞	0.72 X/X_R	15.0
		0.72 X/X_R	∞

$$p_u = \begin{cases} 3c + \gamma X + J\left(\frac{cX}{D}\right) \\ \\ 9c \quad (\text{for } X \geq X_R) \end{cases} \tag{6}$$

$$\mathrm{X}_R = \frac{6D}{\frac{\gamma D}{c} + J} \tag{7}$$

$$\mathrm{y_c} = 2.5\varepsilon_c D \tag{8}$$

The *p–y* curve for sandy soil can be calculated from Eq. (9). k, H, and A are initial foundation reaction factor, penetration depth of pile, and a factor for repetitive load and static load, respectively.

$$p = Ap_u tanh\left[\frac{kHy}{Ap_u}\right] \tag{9}$$

$$A = \begin{cases} 0.9 \quad (\text{for cyclic loading}) \\ \\ \left(3 - 0.8\frac{H}{D}\right) \geq 0.9 \quad (\text{for static loading}) \end{cases} \tag{10}$$

The ultimate bearing force can be obtained from Eq. (11) using the minimum of the calculated p_{us} and p_{ud}.

$$p_u = \begin{cases} p_{us} = (C_1 H + C_2 D)\gamma H \\ \\ p_{ud} = C_3 D\gamma H \end{cases} \tag{11}$$

where the constants C_1, C_2, and C_3 for the ultimate bearing strength and the initial foundation reaction factor, which is used for the *p–y* curve, can be estimated using the internal friction angle (ϕ') in Figs. 2 and 3(API, 2007). In addition, tangential stiffness of soil on pile and pile tip stiffness are also considered by using the so called t-z and q-z curves

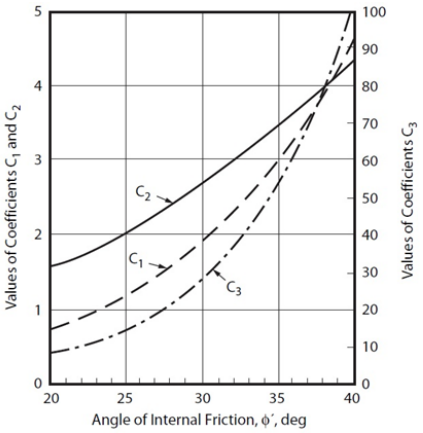

Fig. 2 Coefficients according to phi

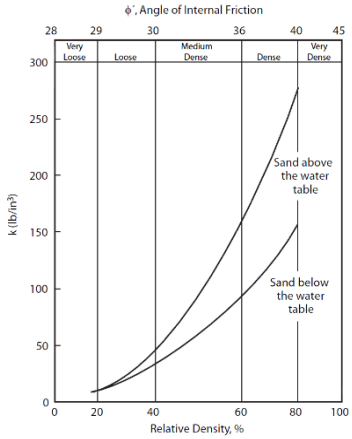

Fig. 3 Initial modulus of subgrade reaction

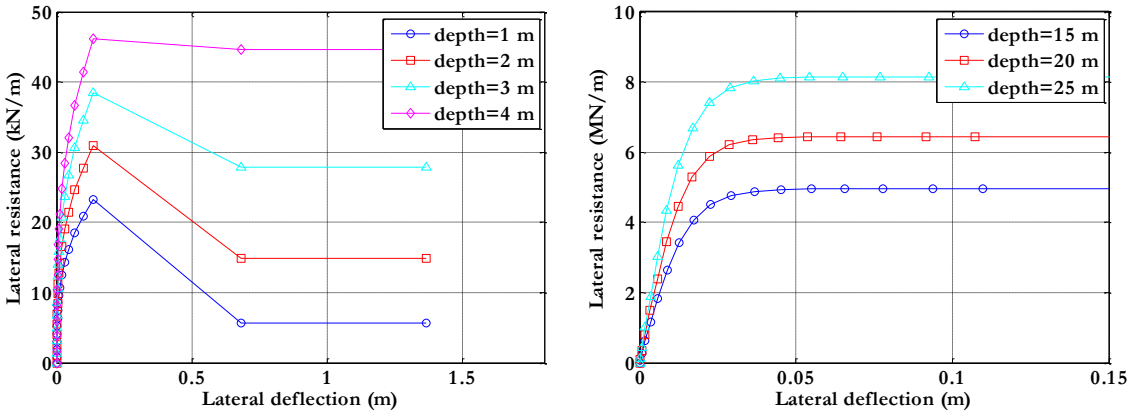

(a) Clay layer (b) Sand layer

Fig. 4 p-y curves for soils

Fig. 4 shows several relations between the loads and the displacements according to the soil properties.

3.1.2 Added mass

In this study, the added mass method proposed by Goyal and Chopra (1989) was used to consider the interaction of structure with seawater. The estimated added mass is regarded as a mass element. Eqs. (12) and (13) show how to calculate the added mass on both the outside (m_a^{o}) and inside (m_a^{i}) of the structure. Here, z, ρ_w, r_{o}, r_{i}, H_{o}, and H_{i} are total length immersed in the water, specific weight of the seawater, outer and inner diameter of the support structure, outer and inner height of the support structure, respectively. a_m is expressed as $(2m-1)\pi/2$. By inserting E_m and D_m in Eqs. (14) and (15) into Eqs. (12) and (13), the added mass can be obtained. K_n is a Bessel function of the second kind of order n, and I_n is a Bessel function of the first kind of order n.

$$m_a^o = (\rho_w \pi r_o^2)\left\{\frac{16}{\pi^2}\frac{H_o}{r_o}\sum_{m=1}^{\infty}\left[\frac{(-1)^{m-1}}{(2m-1)^2}E_m\left(a_m\frac{r_o}{H_o}\right)cos\left(a_m\frac{z}{H_o}\right)\right]\right\} \tag{12}$$

$$m_a^i = (\rho_w \pi r_i^2)\left\{\frac{16}{\pi^2}\frac{H_i}{r_i}\sum_{m=1}^{\infty}\left[\frac{(-1)^{m-1}}{(2m-1)^2}D_m\left(a_m\frac{r_i}{H_i}\right)cos\left(a_m\frac{z}{H_i}\right)\right]\right\} \tag{13}$$

$$E_m\left(a_m\frac{r_o}{H_o}\right) = \frac{K_1\left(a_m\frac{r_o}{H_o}\right)}{K_0\left(a_m\frac{r_o}{H_o}\right)+K_2\left(a_m\frac{r_o}{H_o}\right)} \tag{14}$$

$$D_m\left(a_m\frac{r_i}{H_i}\right) = \frac{I_1\left(a_m\frac{r_i}{H_i}\right)}{I_0\left(a_m\frac{r_i}{H_i}\right)+I_2\left(a_m\frac{r_i}{H_i}\right)} \tag{15}$$

The added mass by pressure on the outer and inner surfaces of the pile and bracing is shown in Fig. 5. The total added mass of the seawater is listed in Table 2.

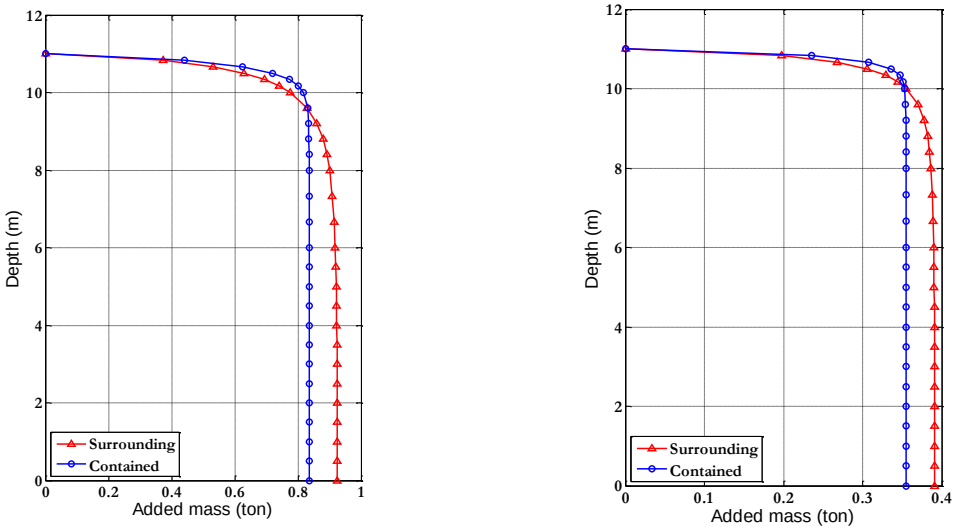

(a) Pile (b) Bracing

Fig. 5 Hydrodynamic added mass on jacket type substructure

Table 2 Added mass according to water depth

Water depth (m)	Added mass (kg)	
	Pile	Bracing
11.00	5.64×10^{-12}	3.39×10^{-12}
10.30	1484.52	681.07
8.24	1730.52	739.99
6.18	1752.39	744.21
4.12	1758.10	745.23
2.06	1760.07	745.58
0.00	1760.57	745.67

3.1.3 Seismic load

Before performing the reliability analysis, the probability distribution of each variable should be estimated. The seismic intensities according to return periods in Korea are proposed in the Korean Port and Harbor Design Standard (MOMAF, 2005). The HeMOSU-1, which was installed by Korea Electric Power Corporation, is under operation for wind energy resource investigation and design load computation of the South-East offshore wind farm development. This area is expected to be a future installation site of the wind power facility. The latitude and longitude by World Geodetic System (WGS84) of the site are 126° 07′ 45.30″ and 35° 27′ 55.17″, respectively. Figure 6 shows the hazard map for the return period of 500 years (MOMAF, 2005). From the hazard map, the peak ground accelerations (PGAs) are estimated and listed in Table 3.

The probability distribution of the seismic factor assumed to follow the three-parameter Weibull distribution as Eq. (16). It can be estimated by using the scale parameter (σ), shape parameter (k), location parameter (μ), and maximum ground acceleration per average return period. The parameters of the probability distribution can be obtained from the relationship between the return period (T) and seismic factor (K_h^T). F_{K_h} is a cumulative probability distribution of the three-parameter Weibull distribution.

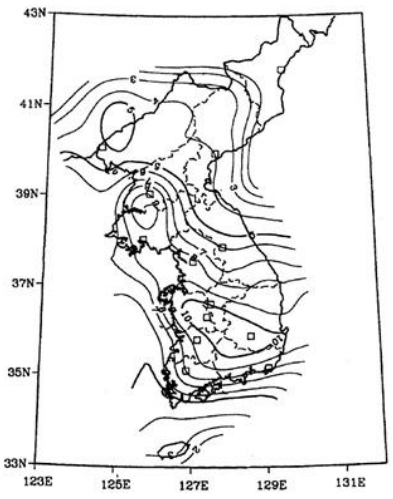

Fig. 6 Seismic hazard (return period – 500 year)

Table 3 Peak ground accelerations at site

Average return period (*year*)	Excess probability/period (*year*)	Peak ground acceleration (g)
50	10% / 5	0.010
100	10% / 10	0.030
200	10% / 20	0.045
500	10% / 50	0.060
1000	10% / 100	0.080
2400	10% / 250	0.110
4800	10% / 500	0.145

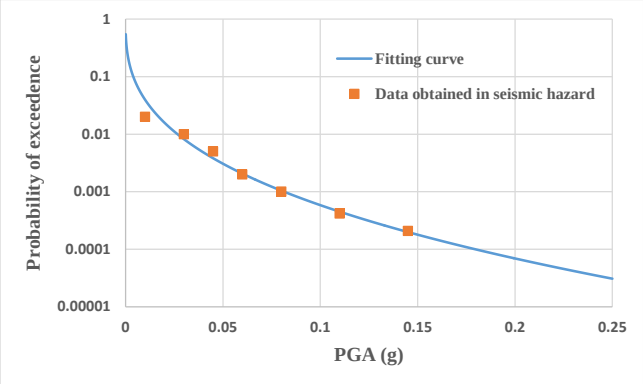

Fig. 7 Estimated probability of exceedance for PGA

$$F_X(x) = 1 - \exp\left[\left(\frac{x-c}{b}\right)^k\right] \tag{16}$$

$$K_h^T = F_{K_h}^{-1}(1 - \frac{1}{T}) \tag{17}$$

$$K_h^T = b(\ln(T))^{1/k} \tag{18}$$

From the regression analysis, the parameters of Eq. (18) are obtained as $\sigma = 4.001 \times 10^{-4}$, $k = 0.3636$, and $\mu = 0$. Fig. 7 shows the exceeding probabilities according to PGAs.

The measured seismic time history data are required because a dynamic analysis must be performed to determine peak response factor. However, the measured data are not available for the site and a relevant artificial earthquake time history was generated. Abundant data are required to estimate the distribution of the peak response factor; therefore, 50 seeds of each PGA from Table 3 were applied to generate 350 seismic ground accelerations in total. Figure 8 shows a typical example of the seismic time history of which PGA is 0.01 g.

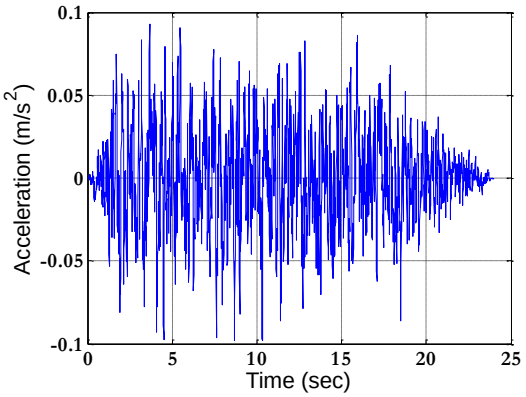

Fig. 8 Time history of seismic acceleration (PGA – 0.01 g)

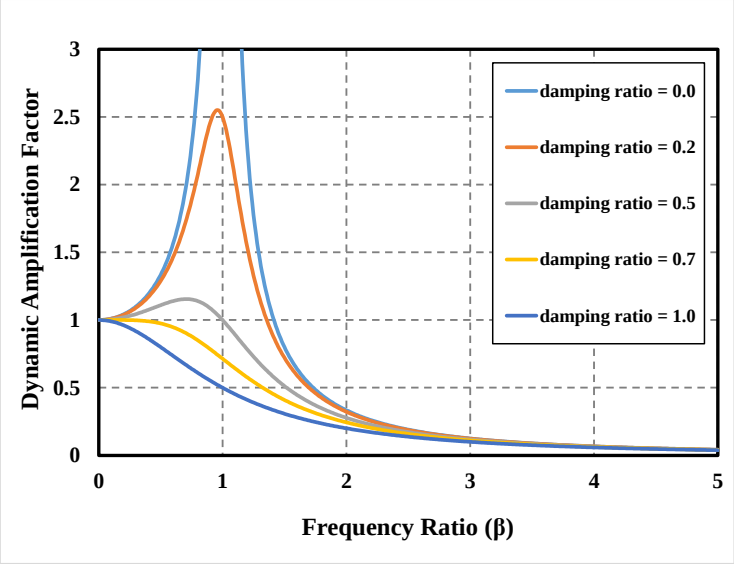

Fig. 9 Dynamic amplification factor (DAF)

3.2 Dynamic amplification

An eigenvalue analysis was performed to get the natural frequencies of the structure. The natural frequency and the mass participation ratio of the first mode are 0.2645 Hz and 63.52%, respectively. The forcing frequency varied in the range between 1.3 and 3.7 according to the seeds. Therefore, the frequency ratio ranged from 5 to 13. As shown in Figure 9, the dynamic amplification factor (DAF) corresponding to the frequency ratio of 5 to 13 can be less than one.

Both DAF and PRF show amplification of structural response under dynamic load. The difference between the two factors is that DAF is defined in linear single degree of freedom (SDOF) system while PRF in nonlinear multi-degree of freedom (MDOF) system. PRF can be understood as the superposition of DAFs in MDOF system. But, it is not simple superposition of DAF since PRF includes both the random loads and the nonlinear response effects. The definition of PRF is quite empirical rather than theoretical.

3.3 Probability distribution of the peak response factor

The distribution of the peak response factor can be obtained by the dynamic peak response from dynamic analysis and by the static response from static analysis. According to the displacement response, the three-parameter Weibull distribution is the most suitable distribution, as shown in Fig. 10. The histogram and probability density function of the peak response factor are shown in Fig. 11.

As shown in the probability density, the position parameter of the *x*-axis peak response factor is 0.3296. As shown in Fig. 9, when the frequency ratio is high, the position parameter of the peak response factor can be lower than 1.0. A real earthquake, whose main frequencies are usually distributed in a low range, may produce a bigger amplification effect than an artificial earthquake.

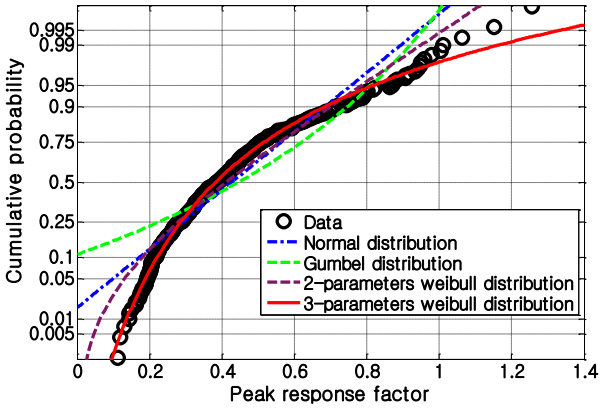

Fig. 10 Probability plot for PRF

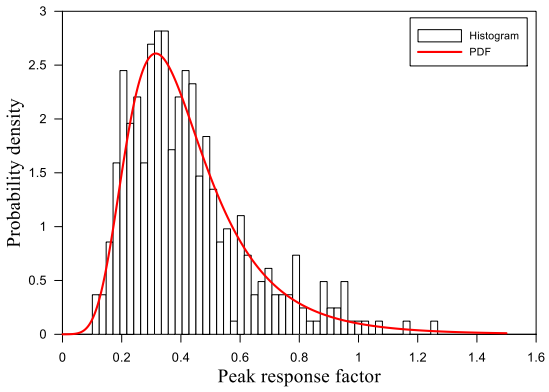

Fig. 11 Histogram and PDF of PRF

Table 4 Characteristics of random variables

Random variables	Probability distribution	Characteristic value
Coefficient of earthquake (K_h)	3-parameters Weibull	k = 0.3636, σ = 4.001× 10^{-4}, μ = 0
Peak response factor (R_n)	3-parameters Weibull	k = 0.1068, σ = 0.1419, μ = 0.3296
Specific weight of clay (γ_c)	Log-normal	λ = 2.8511, ξ = 0.1492
Specific weight of sand (γ_s)	Log-normal	λ = 2.8792, ξ = 0.1492
Internal friction angle (ϕ `)	Beta	q = r = 1.5825
Undrained shear strength (c_u)	Log-normal	λ = 2.0467, ξ = 0.2558

3.4 Reliability analysis

The seismic load and the soil properties are considered as random variables in the reliability analysis. The distribution of variables and the parameters is listed in Table 4. The FORM, Level II reliability analysis method was applied.

The internal friction angle of sandy soil can be calculated by curve fitting using Figs. 2 and 3. In the reliability analysis, if the calculation result is out of range of the internal friction angle, an inappropriate initial foundation reaction factor may be produced. To prevent this erroneous result, the internal friction angle is assumed to follow the Beta distribution and 30° and 40° were set as lower and upper limits. In previous research, the normal distribution was used for soil properties (Yoon *et al*. 2013, Yoon *et al*. 2014), but the soil property cannot be zero or a negative number. If the sensitivity of the soil property is very high, the most probable failure point can be dramatically high or low, even become negative ones in case of acting as resistance. Thus, the log normal distribution was used in this study, and the three-parameter Weibull distribution was used for the seismic factor and peak response factor. The allowable horizontal displacement (R_{all}) is 25 mm according to the Technics of Road Design (Korea Road Association, 2009).

By using the response surface method, the limit state function was defined as Eq. (19). A sample point for estimation of the response surface was obtained using the SD method.

$$g(X) = R_{all} - R_n R_{st}(K_h, \gamma_{clay}, \gamma_{sand}, \phi', c_u) \tag{19}$$

A Level III reliability analysis was performed to verify the result of the Level II analysis. In the existing MCS method, 10–100 times the inverse of the expected failure probability is used as a sample number. If an estimated failure probability is very low, dynamic structural analysis based MCS is very hard to apply because of calculation time. Therefore, the LHS with dynamic structural analysis was conducted.

3.5 Analysis results

LHS result showed reliability index of 3.3481 as shown in Fig. 12. The reliability index by FORM with peak response factor resulted in 3.2012 within 4 iterations, which is 6.8428×10^{-2}% in probability of failure. When the peak response factor was not considered as random variable, the reliability index was 2.8693 which corresponds failure probability of 2.0569×10^{-1}%. The convergence curves are shown in Fig. 13. Table 5 compares the error in reliability index and computation time of the two approaches, and MPFPs with and without considering PRF as random variable are shown in Table 6.

A 64-bit Windows 7 operating system with 3.4-GHz quad core CPU and 16-GB RAM was used for the analysis. The run-time was 6 minutes and 30 seconds for FORM, 21 days 20 hours and 30 minutes for LHS.

Table 5 Reliability index

	LHS	FORM with PRF
Reliability index	3.3481	3.2012
Relative error	-	4.3876%
Computational time	21 days 20 hours 30 minutes	6 minutes 30 seconds

Table 6 MPFPs and sensitivity factors (FORM)

Random variables	Case 1 (PRF as variable)		Case 2 (PRF as constant)	
	MPFPs	Sensitivity factors	MPFPs	Sensitivity factors
Coefficient of earthquake (K_h)	0.0760 g	-0.9495	0.0601 g	-0.9998
Peak response factor (R_n)	0.6046	-0.3136	-	-
Specific weight of clay (γ_c)	17.3898 kN/m^3	8.1293×10^{-3}	17.3536 kN/m^3	2.0707×10^{-2}
Specific weight of sand (γ_s)	17.9126 kN/m^3	3.4023×10^{-7}	17.9126 kN/m^3	6.5059×10^{-6}
Internal friction angle (ϕ`)	34.9939 °	4.2348×10^{-4}	34.9897 °	1.0674×10^{-3}
Undrained shear strength (c_u)	7.7414 kPa	1.8480×10^{-4}	7.7399 kPa	4.6793×10^{-4}
Reliability index	3.2012		2.8693	

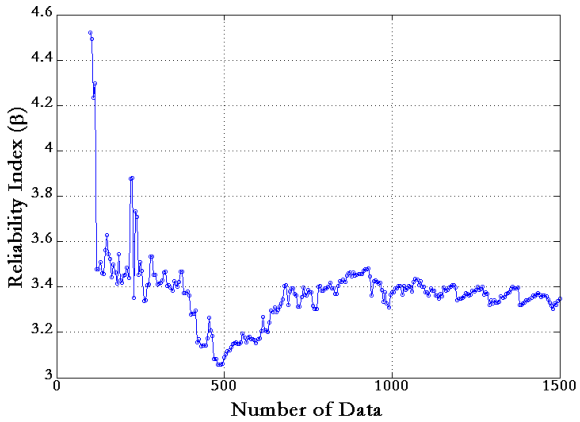

Fig. 12 Convergence of reliability index using LHS without PRF

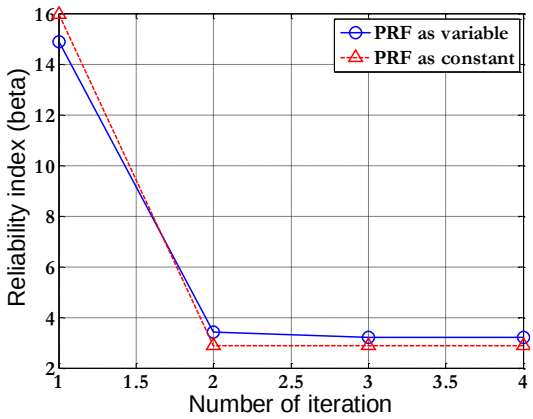

Fig. 13 Convergence of reliability index using FORM

4. Conclusions

The reliability analysis of a jacket-type offshore wind turbine support structure was shown by using a new random variable called peak response factor. Using the factor, the dynamic amplification effect can be considered in reliability analysis of offshore wind turbine support structure. Reliability index by the proposed method shows small error compared with LHS result. However, computational time was innovatively reduced. It took 21 days and more by conventional LHS but only 6 minutes by the proposed method. To check the effect of PRF on failure probability, numerical analysis with and without considering PRF as random variable was done. Result showed that failure probability might be over-estimated if PRF is assumed as constant. Numerical result also showed that the seismic response is the most sensitive random variable and PRF is the second one. Among all random variables, these two random variables seem to be dominant ones.

Acknowledgements

This research was conducted with funding from Korea Institute of Energy Technology Evaluation and Planning (KETEP) with the help of the Ministry of Trade, Industry & Energy (MOTIE) (No. 20123030020110) and was also supported by the Human Resources Development of the KETEP grant funded by MOTIE (No. 20144030200590).

References

American Petroleum Institute (API) (2007), *Recommended Practice for Planning, Design and Constructing Fixed Offshore Platforms Working Stress Design*, API Publishing Services.

ANSYS Inc. (2009), ANSYS 12.0 user's Guide, Canonsburg, PA, USA.

Box, G.E.P. and Wilson, K.B. (1951), "On the experimental attainment of optimum conditions", *J. R. Stat. Soc*., **13**, 1-38.

Bucher, C.G. and Bourgund, U. (1987), *Efficient use of response surface methods*, Report No. 9-87, Institute fur Mechanics, University of Innsbruck, Innsbruck, Austria.

Bush, E. and Manuel, L. (2009), "Foundation Models for Offshore Wind Turbines", 47th AIAA Aerospace Sciences Meeting Including the New Horizons Forum and Aerospace Exposition, Orlando, Florida, 1-7.

Choi, E.J., Han, C.W., Kim, H.J. and Park, S.H. (2014), "Optimal design of floating substructures for spar-type wind turbine systems", *Wind Struct*., **18**(3), 253-265.

Ministry of Maritime Affairs and Fisheries (MOMAF) (2005), *Engineering Standards Commentaries Port and Harbor Facilities*, Ministry of Oceans and Fisheries, Korea.

Nava, V., Failla G., Arena, F. and Santini, A. (2014), "On the fatigue behavior of support structures for offshore wind turbines", *Wind Struct*., **18**(2), 117-134.

Goyal, A. and Chopra, A. (1989), "Simplified evaluation of added hydrodynamic mass for intake tower", *J. Eng. Mech. - ASCE*, **115**(7), 1393-1435.

Haldar, A. and Mahadevan, S. (2000), *Reliability assessment using stochastic finite element*, John Wiley, New York.

Hasofer, A.M. and Line, L.C. (1974), "Exact and invariant second moment code format", *J. Eng. Mech. Div. - ASCE*, **100**, 111-121.

Jonkman, J., Butterfield, S., Musial, W. and Scoot, G. (2009), *Definition of a 5-MW reference wind turbine for offshore system development*, NREL/TP-500-38060.

Khuri, A.I. and Cronell, J.A. (1987), *Response Surfaces:Design and analysis*, Dekker, New York.

Korea Road Association (2009), *The Technics of Road Design. the third volume*, Korea Expressway Corporation, gim cheon.

Lee, S.G. and Kim, D.H. (2011), "Reliability analysis of pile type quaywall using response surface method", *J. Korean Soc. Coastal Ocean Eng*., **23**(6), 407-413.

Lee, S.G. and Kim, D.H. (2014), "Reliability analysis offshore wind turbine support structure under extreme ocean environmental loads", *J. Korean Soc. Coastal Ocean Eng.*, **26**(1), 33-40.

Rackwitz, R. and Fiessler, B. (1978), "Structural reliability under combined random load sequences", *Comput. Struct*., **9**(5), 489-494.

Schueller, G.I., Bucher, C.G., Bourgund, U. and Ouypornpasert, W. (1987), *On Efficient Computational Schemes to Calculate Structural Failure Probabilities*, Stochastic Structural Mechanics, U.S.-Austria Joint Seminar, 338-410.

Yi, J.H., Kim, S.B., Yoon, G.L. and Andersen, L.V. (2015), "Influence of pile-soil interaction on the dynamic properties of offshore wind turbines supported by jacket foundations", *Proceedings of the 2015 International Ocean and Polar Engineering Conference*, 285-288.

Yi, J.H., Yoon, G.L. and Li, Y. (2014), "Numerical investigation on effects of rotor control strategy and wind data on optimal wind turbine blade shape", *Wind Struct*., **18**(2), 195-213.

Yoon, G.L., Kim, K.J. and Kim, H.Y. (2013), "Reliability analysis of monopile for a offshore wind turbine using response surface method", *J. Korean Soc. Civil Engineers*, **33**(6), 2401-2409.

Yoon, G.L., Kim, S.B., Kwon, O.S. and Yoo, M.S. (2014), "Partial safety factor of offshore wind turbine pile foundation in west-south mainland sea", *J. Korean Soc. Civil Engineers*, **34**(5), 1489-1504.

Zhang, J., Yugang, L. and Higui, K. (2010), "Application of DSI techniques to monopile foundations of offshore wind turbines reliability problems", *Electronic J. e-Geotech. Geoenviron. Eng*., **15**, 1-9.